# Recessive Mutations in a Common Pathway Block Thymocyte Apoptosis Induced by Multiple Signals

**Francis A. Flomerfelt and Roger L. Miesfeld*‡§**

*Departments of Molecular and Cellular Biology, ‡Biochemistry, and §The Arizona Cancer Center, University of Arizona, Tucson, Arizona 85724

***Abstract.*** The glucocorticoid receptor (GR) is a ligand-regulated transcription factor that controls genes necessary to initiate glucocorticoid-induced thymocyte apoptosis. We have performed a genetic analysis of thymocyte cell death by isolating and characterizing a panel of $GR^+$ dexamethasone-resistant mutants of the murine WEHI7.2 thymocyte cell line. These apoptosis-defective ($Apt^-$) mutants were used to identify previously unknown early steps in the apoptotic pathway. The $Apt^-$ mutants contain nonglucocorticoid receptor, recessive mutations in genes that represent multiple complementation groups. These mutations block apoptosis induced by dexamethasone, gamma irradiation, and c-AMP treatment before the point where Bcl-2 exerts its protective effect. We propose that different signals share a common apoptotic pathway, and that the induction of apoptosis involves multiple precommitment steps that can be blocked by recessive mutations.

APOPTOSIS is a common, cell autonomous process in which a cell actively participates to cause its own death in response to a variety of signals (14, 35, 38, 59, 70). In mammals, for example, apoptosis serves an important role in the proper development and maintenance of the hematopoietic (36), immune (15, 26, 52), and neural systems (33, 50). The widespread occurrence of apoptosis in multicellular organisms suggests that it is an important biological process. Recent findings underscore this idea by implicating the failure to initiate, or the inappropriate induction of apoptosis, in several pathological conditions (3, 11, 22).

The active nature of apoptosis is illustrated by the series of sequential events that characterize this type of cell death. Apoptotic cells undergo a series of dramatic morphological changes before loss of viability. These include chromatin aggregation, nuclear and cytoplasmic condensation, and finally, fragmentation of the cell into small membrane bound apoptotic bodies that can contain nuclear fragments and intact organelles (42, 70). In addition, multiple cellular responses can accompany morphological changes. These include the induction of select genes (61), changes in cytoplasmic $Ca^{++}$ levels (44, 48), and degradation of genomic DNA (1, 69).

Numerous signals can trigger apoptosis and several of these may be active in any given cell type. For example, immature murine thymocytes undergo apoptosis in response to glucocorticoids (62) and T cell receptor (TCR)[1] stimulation (65). More recently, it has become apparent that damaged or impaired cells can produce an apoptotic signal (11, 47). For instance, damaging agents such as oxidative stress (8, 31), low dose gamma irradiation (15), and some chemotherapeutic drugs (29) can cause thymocyte apoptosis. Less obvious types of damage, such as mutations that result in inappropriate gene expression, may also produce an apoptotic signal. For example, enforced expression of *c-myc* in serum-starved fibroblasts causes cell death (21). Similarly, elevated expression of the tumor-suppressor gene, p53, in proliferating myeloid cells triggers apoptosis (71).

While multiple stimuli can trigger apoptosis, there are fewer known cellular antagonists of this process. An example is Bcl-2, identified by cloning the t[14:18] chromosome translocation in follicular lymphoma (13), that developmentally blocks apoptosis in several cell types (30, 34, 63). In thymocytes, ectopic Bcl-2 expression also blocks apoptosis initiated by glucocorticoids, gamma irradiation, TCR stimulation (63, 67), and $H_2O_2$ (31). This data suggests that Bcl-2 antagonizes an event that is a common response to a variety of apoptotic triggers. Recent data has implicated the generation of reactive oxygen species (31, 34) or calcium mobilization (39) as late events antagonized by Bcl-2. However, while early apoptotic signals, and late events antagonized by Bcl-2,

Please address all correspondence to Dr. Roger L. Miesfeld, Department of Biochemistry, Arizona Cancer Center, University of Arizona, Tucson, AZ 85724. Tel.: (602) 626-2343. Fax: (602) 626-2284.

1. *Abbreviations used in this paper*: CBS, calf bovine serum; Cam, calmodulin; dex, dexamethasone; $dex^r$, dex-resistant; FACS, fluorescent-activated cell sorting; GR, glucocorticoid receptor; GST, glutathione-S-transferase; ICE, interluekin-1 β-converting enzyme; PD, phosphate; TCR, T cell receptor.

have received intensive study, intervening steps in the apoptotic pathway that link the two have remained obscure.

To investigate the mechanism controlling the induction of cell death, apoptosis-defective ($Apt^-$) mutant cell lines were isolated and characterized in this study. We chose to investigate glucocorticoid-induced apoptosis in the murine cell line WEHI7.2 (W7.2), which is a tissue culture model for immature thymocytes (15, 28). W7.2 cells have extremely low levels of Bcl-2 (19, 39) and undergo apoptosis in response not only to the synthetic glucocorticoid agonist, dexamethasone (dex) (16), but also to cAMP analogs, $H_2O_2$, calcium ionophore (46), and gamma irradiation (57). The low incidence of spontaneous dex resistance ($<1 \times 10^{-10}$) in W7.2 cells (19) provided a powerful means to clonally isolate dex-resistant ($dex^r$) mutants after chemical mutagenesis. Furthermore, W7.2 cells are particularly useful for somatic cell genetic studies since they have a nearly normal diploid karyotype with a stable mean chromosome number of 43. Biochemical and genetic analyses of the $Apt^-$ mutants have helped to clarify early steps in thymocyte apoptosis and have led to a proposed model that describes a common apoptotic pathway.

## Materials and Methods

### Cell Culture and Reagents

Cells were grown in DMEM (Irvine Scientific, Santa Ana, CA) containing 10% iron-supplemented, defined calf bovine serum (CBS, Hyclone Labs., Logan, UT), 100 U/ml penicillin, and 0.1 mg/ml streptomycin in an atmosphere of 90% humidity, 8% $CO_2$ at 37°C. Isotonic phosphate (PD) buffer contained 136 mM NaCl, 2.6 mM KCl, 1.5 mM $KH_2PO_4$, and 8.1 mM $Na_2HPO_4$. Isolation of clonal cell lines by soft agar cloning (17) included addition of the appropriate drugs where indicated. The cell line Apt4.8 was designated W.408 in a previous publication (23). WG3 and WG5 were grown in media containing 10% charcoal-stripped CBS. For all treatments used to induce apoptosis, a dose response experiment was done using W7.2 cells, and the lowest treatment level that caused cell death was used for all subsequent experiments. Growth curves were done by treating cells at a density of $10^5$ to $3 \times 10^5$ cells/ml, and using an hemocytometer to count viable cells by trypan blue (GIBCO BRL, Gaithersburg, MD) exclusion at various intervals. Dexamethasone (Sigma Chem. Co., St. Louis, MO) was prepared as a 0.01-M stock dissolved in ethanol. 8-bromo-c-AMP (Alderidge) was dissolved in water at 200 mM and used at a final concentration of 200 μM. Gamma irradiation was delivered from $^{60}Co$ source from an Atomic Energy of Canada Theratron 60 at variable dosage rates of 70–80 rads/min. $H_2O_2$ and calcium ionophore A23187 (dissolved in DMSO at 4.0 mM), were obtained from Sigma and used at a final concentration of 100 μM and 1.5 μM, respectively. G418 (GIBCO BRL) was dissolved in 0.1 M Hepes, pH 7.2, and active drug was used at a concentration of 1,000 μg/ml. Wright-Giemsa reagents were purchased from Sigma and were used as recommended. 5-Iodoacetamidofluorescen and 5-and-6-Iodoacetamidotetra-methylrhodamine (Research Organics, Inc., Cleveland, OH) were dissolved in DMSO as a 1-mg/ml stock. Gas chromatography grade PEG 4000 was obtained from EM Science (Cherry Hill, NJ).

### Mutagenesis Protocol

Cell cultures were grown to a density of $2.5 \times 10^5$ cells/ml and treated with 300–400 μg/ml ethyl methanesulfonate (EMS) for 13 h which killed 50% of treated cells. To isolate dex-resistant cell lines, EMS-treated cells (in some experiments cells were treated concurrently with 1 μM dex) were washed and allowed to recover in DMEM containing 10% CBS and antibiotics for 2–3 d. These cells were then plated in soft agar media containing 1 μM dex (G418 was added for WG3 and WG5 mutagenesis). Colonies were picked and expanded in DMEM containing 10% CBS, $10^6$ M dex, and antibiotics. The origin of the mutants was as follows: Apt4.8 and Apt4.19 were derived W7.2 in separate experiments using 400 μg/ml EMS, Apt3.8 was also derived from W7.2 but 300 μg/ml EMS was used in the presence of dex. Apt5.N mutants were all derived from WG5 using 400 μg/ml EMS; Apt5.8 and Apt5.26 were isolated from the same experiment, while Apt5.45, Apt5.60, and Apt5.100 were isolated from three separate experiments.

### Dex Binding

Routinely, $5 \times 10^7$ cells were harvested, washed once with PD buffer, frozen in liquid nitrogen, and stored at −80°C. Cell pellets were thawed on ice and 250 μl ice cold TEGN50 (10 mM Tris-HCl, pH 7.5, 1 mM EDTA, 10% vol/vol glycerol, 1 mM 2-mercaptoethanol, 50 mM NaCl, 10 mM $Na_2MoO_4$, 1 mM PMSF) was immediately added. Each sample was sonicated on an ice/$H_2O$ slurry and cleared by centrifugation in a 4°C microfuge at maximum speed for 5 min. Triplicate-binding reactions were assembled by adding [$^3$H]dex (Amersham, 12.4 mM stock concentration) to each tube (final concentration = 10 nM) which contained 65 μl of cell extract normalized for protein content. To measure nonspecific binding, unlabeled dex (final concentration = 10 μM) was added to one tube. The labeling reactions were incubated on ice for 90 min. To remove unbound ligand, 100 μl of dextran-coated charcoal suspension (10 mg/ml acid-activated charcoal and 1 mg/ml dextran in TEGN 50) was added to each tube and vortexed briefly. The entire binding reaction was transferred into the top portion of a 0.45 μm Micro-Spin Filter (Lida Manufacturing) and centrifuged at 50% maximum speed in an Eppendorf microfuge for 5 min at room temperature. Bound [$^3$H]dex in the charcoal-free filtrate was measured in a scintillation counter (Beckman Instrs.). Net specific binding was calculated by subtracting the nonspecific binding from the average of the duplicate reaction tubes.

### Transient Heterokaryon Assay

Cells were grown to a density of ~$5 \times 10^5$/ml, harvested by centrifugation, washed in isotonic PD buffer, and resuspended at $5 \times 10^7$ cells/ml in DMEM containing 0.5% CBS. Cells were labeled by addition of either 5-Iodoacetamidofluorescen (final concentration = 0.075 μg/ml) or 5-and-6-Iodoacetamidotetra-methylrhodamine (final concentration = 1.0 μg/ml) and incubated at 37°C for 30 min. Labeled cells were washed three times in 37°C serum-free DMEM to remove residual label and serum. At least $10^9$ cells of each fusion partner were mixed in 37°C serum-free DMEM in a 50-ml Falcon tube, pelleted at 400 *g*, and the supernatant was completely removed by aspiration. The pellet was tapped to loosen the cells and 1.0 ml of prewarmed (42°C) fusagen (45% PEG 4000, and 5% DMSO in PD buffer) was added dropwise over a period of 1 min while swirling the tube. The tube was quickly transferred to a 42°C water bath and swirled for thirty seconds, and then placed in a tabletop centrifuge (prewarmed to 37°C) and spun for 10 s at 400 *g* (60 s total). Fused cells were then diluted dropwise with 42°C serum-free DMEM as follows: 1.0 ml in 30 s, 3.0 ml over 30 s, and 20 ml over 1 min. Cells were allowed to settle for 5 min, and then spun at 400 *g* for 10 min and gently resuspended in 37°C serum-free DMEM. This wash was repeated to remove residual PEG and the cells were resuspended at a density of $5 \times 10^6$ cells/ml in DMEM with 10% serum, and allowed to recover for 2–4 h at 37°C. The cell suspension was adjusted to 35 ml and layered over a 15-ml Ficoll-Paque gradient (Pharmacia LKB Biotechnology, Piscataway, NJ) and centrifuged at 500 *g* for 30 min at 15°C. The live cells were removed from the interface, washed twice with 37°C PD buffer, and brought to a final density of $3 \times 10^6$ cells/ml before sorting on a FACStar instrument (Beckman Instrs., Fullerton, CA). Fused cells were sorted based on fluorescent emissions, forward, and side scatter in order to purify doubly labeled, large, and viable cells. Sorted double positive cells were concentrated by centrifugation and suspended in DMEM containing 1.0% CBS ±1 μM dex. These samples were then placed in an incubator and analyzed by microscopic examination at 1-, 3-, and 5-d intervals. The difference in viability between the control and dex-treated samples was determined by comparing the number of light fractile cells using a phase contrast microscope as described (16).

### Stable Transfectants

DNA to be transfected was linearized in the β-lactamase gene with either AccI or XmnI restriction enzyme, phenol extracted, ethanol precipitated, and resuspended in water. Cells were grown to a density of $3–5 \times 10^5$ cells/ml, harvested by centrifugation, washed once with PD buffer, and resuspended at a density of $10^7$ cells/ml in HBS buffer (21 mM Hepes, 137 mM NaCl, 5 mM KCl, 0.7 mM $Na_2HPO_4$, 6 mM glucose). Equal amounts

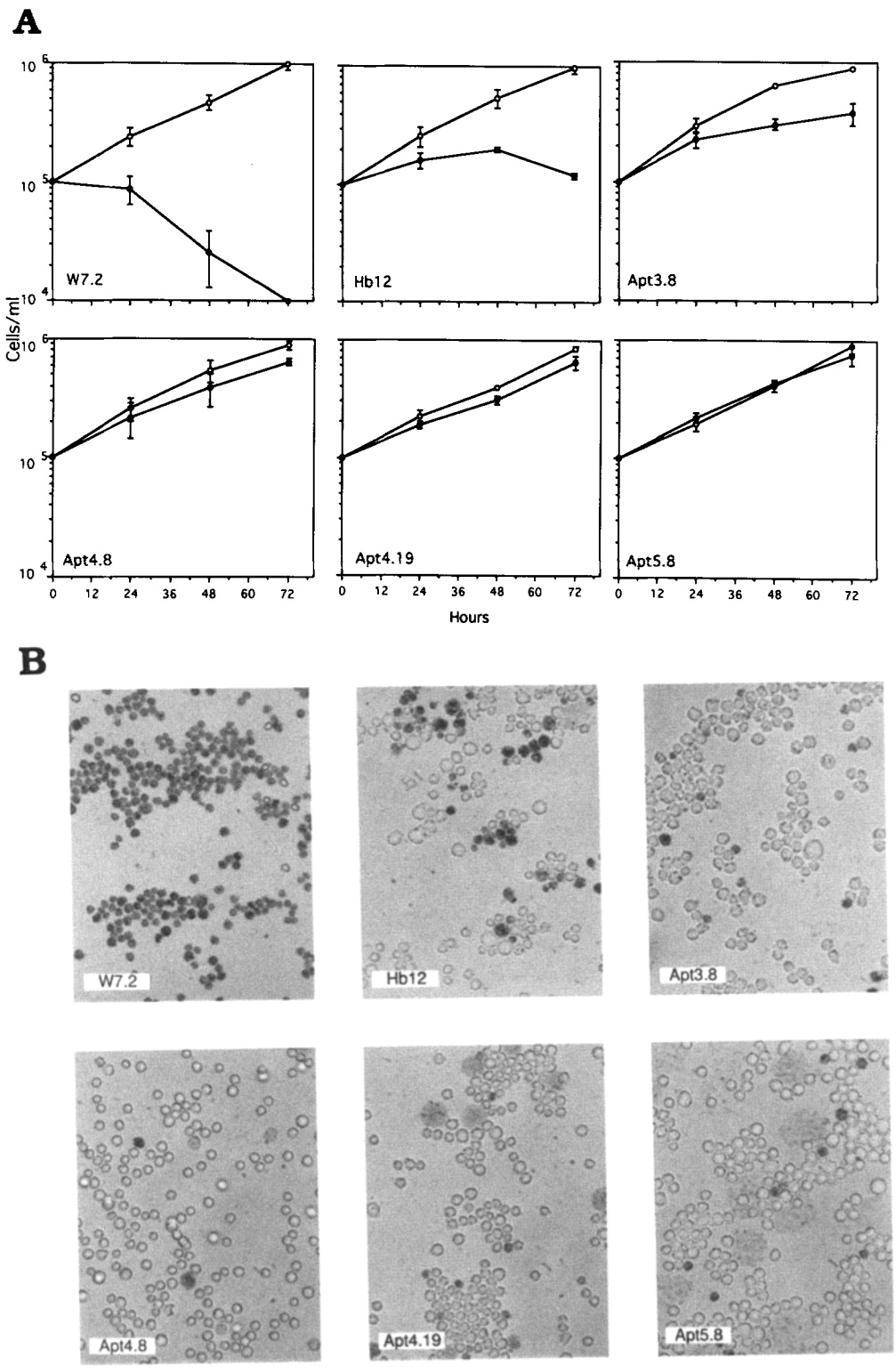


*Figure 1.* Sensitivity of W7.2, Hb12 Apt3.8, Apt4.8, Apt4.19, and Apt5.8 cells to dex. Growth curves (*A*) were derived from triplicate cultures of cells grown in the absence (*open circle*) or presence (*closed circle*) of 0.1 μM dex (*vertical bars* shows standard deviation). Cell viability was determined by trypan blue exclusion. (*B*) Representative fields of trypan blue–stained cells, exposed to dex for 3 d, and photographed through a phase contrast microscope are shown.

of linearized and supercoiled plasmid (100 μg total) were added to 1 ml of cell suspension in an electroporation cuvette. A BRL Cell Porater was used at a setting of 1180 μF and 250 V at room temperature. After a 10-min recovery period, the transfected cells were plated in DMEM containing 10% CBS, and antibiotics. To isolate stable transfectants, the transfected cells were plated in G418-containing media for 1–2 d before being plated in soft agar media containing G418.

## *Northern blots*

Total RNA was isolated by guanidinium lysis followed by CsCl centrifugation and 15 μg of RNA/lane was subjected to Northern analysis as described (2). The Cam probe was an EcoRI–PstI fragment from a chicken genomic clone (56), the GST Ybl probe was a full-length cDNA cloned from rat (10), the Dag-8 probe was the 3′ end of a dex-induced transcript cloned from W7.2

*Table I. Relative Dex Binding and Dex Sensitivity of W7.2 Derivatives and Apt⁻ Mutants*

| | Cell line | Relative dex binding | Dex sensitive |
|---|---|---|---|
| Wild-type cells | W7.2 | 1.0 | yes |
| | WG3 | 1.9 | yes |
| | WG5 | 2.5 | yes |
| Mutant cells | Apt5.8 | 2.0 | no |
| | Apt4.8 | 1.0 | no |
| | Apt3.8 | 1.0 | no |
| | Apt4.19 | 1.0 | no |
| | Apt3.2 | 0.7 | no |
| | Apt3.6 | 0.5 | no |
| | Apt3.80 | 0.1 | no |
| +GR cDNA Apt cells | Apt4.8G8 | 2.5 | no |
| | Apt3.8G3 | 2.0 | no |
| | Apt4.19G5 | 2.0 | no |
| | Apt3.2G2 | 1.9 | yes |

Dex-binding values are the means of at least three separate experiments. Relative values were obtained by the division of specific dex-binding values for each cell line by the dex-binding value of W7.2. Dex sensitivity was evaluated by the ability of cell lines to grow in the presence of 1.0 μM dex for a 4-d period.

(Flomerfelt, F. A., and R. L. Miesfeld, manuscript in preparation), and the histone H3.3 probe used was an internal PCR fragment isolated from W7.2 using H3.3-specific primers (55). Probes were labeled with $^{32}$PαdCTP using a random primer labeling kit (Promega Corp., Madison, WI) and hybridization was done at 42°C in a 50% formamide buffer (2). Blots were washed in buffer containing 0.1× SSC and 0.1% SDS at 65°C. Quantitation of transcript levels was done on a Phosphorimager and included normalization to mouse histone H3.3 expression levels (Molecular Dynamics, Sunnyvale, CA).

### *Microscopy*

False color fluorescent images were produced using a liquid cooled CCD camera (Photometrics) attached to an Olympus IMT-2 inverted microscope equipped with a 60× 1.4 NA Olympus objective. Standard optics for visualization of rhodamine and fluorescein fluorescence were used. The digitized image was processed on a Silicon Graphics Personal Iris computer. Transmitted light micrographs were obtained using standard techniques. Electron microscopy was carried out using established techniques (54).

## *Results*

### *Isolation and Characterization of Dexʳ Cell Lines*

EMS mutagenesis of dex-sensitive W7.2 cell lines, followed by selection for growth in 1 μM dex, resulted in an isolation of several hundred dexʳ cell lines. Fig. 1 shows the effect of dex on the growth of W7.2 and representative dexʳ cell lines Apt3.8, Apt4.8, Apt4.19, and Apt5.8 that were clonally isolated from four separate cultures of mutagenized dex-sensitive cells (see Materials and Methods for parental origins). As a population, the growth of W7.2 cells is slowed for 24 h in response to dex treatment. Individual apoptotic cells, as judged by morphology, are evident within 12 h of treatment (Figs. 1 *B* and 2) and increase in number as culture viability is lost. In comparison, the dexʳ mutant Apt3.8 showed only a slight decrease in growth rate in the presence of dex, while the growth of Apt4.8, Apt4.19, and Apt5.8 was unaffected by hormone. In addition, cultures of these cells retained a high level of viability for three days in dex (Fig. 1 *B*) and could be maintained in media containing dex for several weeks (data not shown).

*Table II. Frequency of Dex Resistance after EMS Mutugenesis of Dex-sensitive Cell Lines*

| Cell line | # Mutagenized | # Dex resistant | # GR⁺ | % Apt⁻ GR⁺ |
|---|---|---|---|---|
| W7.2 | $10^9$ | 90 | 3/90 | <5% |
| WG3 | $3 \times 10^9$ | 22 | 14/22 | ≈65% |
| WG5 | $8.5 \times 10^9$ | 101 | 44/46 | >95% |

GR content was determined as described by either, or combinations of, dex binding, dex-dependent transcriptional regulation of pMMCAT reporter plasmid, or complementation of dex-dependent apoptosis when fused to Apt3.2 cells.

For comparison, the growth of a W7.2 cell line that expresses human Bcl-2, Hbl2 (39), was examined under the same conditions. In agreement with previous results (39), Hbl2 cells remained viable for three days in dex. However, Hbl2 growth was slowed and some apoptotic cells were evident by the third day (Fig. 1 *B*).

### *Identification of Dexʳ Mutants That Have a GR⁺, Apt⁻ Phenotype*

Since previous attempts to obtain dexʳ thymocyte cell lines have often resulted in the isolation of glucocorticoid receptor (GR) defective cells (9, 64), the dexʳ cell lines were screened for dex-binding and transcriptional regulatory activities to identify apoptotic-defective mutants that expressed normal levels of functional GR. Table I shows the results of [³H]dex-binding assays that measured GR levels in selected dexʳ cell lines. The majority of the dexʳ cell lines derived from W7.2 had reduced levels of [³H]dex binding (e.g., Apt3.2, Apt3.6, and Apt3.80). However, some cell lines (Apt4.8, Apt3.8, Apt4.19, and Apt5.8) retained at least wild-type levels of [³H]dex-binding activity. Each of these mutants was tested for dex-dependent GR transcriptional regulatory activity by transient transfection of the GR-responsive reporter plasmid pMMCAT (18), and displayed equal or greater levels of dex-dependent induction of CAT activity than that observed with W7.2 (data not shown). Together, these results indicated that Apt3.8, Apt4.8, Apt4.19, and Apt5.8 have normal levels of functional GR, are not affected by limiting ligand availability, and do not express a dominant negative form of GR.

To exclude the possibility that dex resistance was due to undetected loss-of-function GR mutations, selected dexʳ mutants were stably transfected with a GR cDNA expression plasmid that coexpresses the bacterial neomycin gene (pRGRNeo) (18). G418 resistant subclones of each mutant were isolated, screened for increased [³H]dex-binding activity, and those with the highest levels of dex binding were tested for dex-induced cell death (Table I). Stable expression of GR cDNA restored dex sensitivity to the Apt3.2 subclone Apt3.2G2. This result indicated that the dex resistance of Apt3.2 was due to a GR deficiency. In contrast, subclones of Apt4.8, Apt3.8, and Apt4.19 (Apt4.8G8, Apt3.8G3, and Apt4.19G5, respectively), each contained at least twice the parental level of GR and maintained a dexʳ phenotype (Table I). Therefore, Apt4.8, Apt3.8, and Apt4.19 were desig-

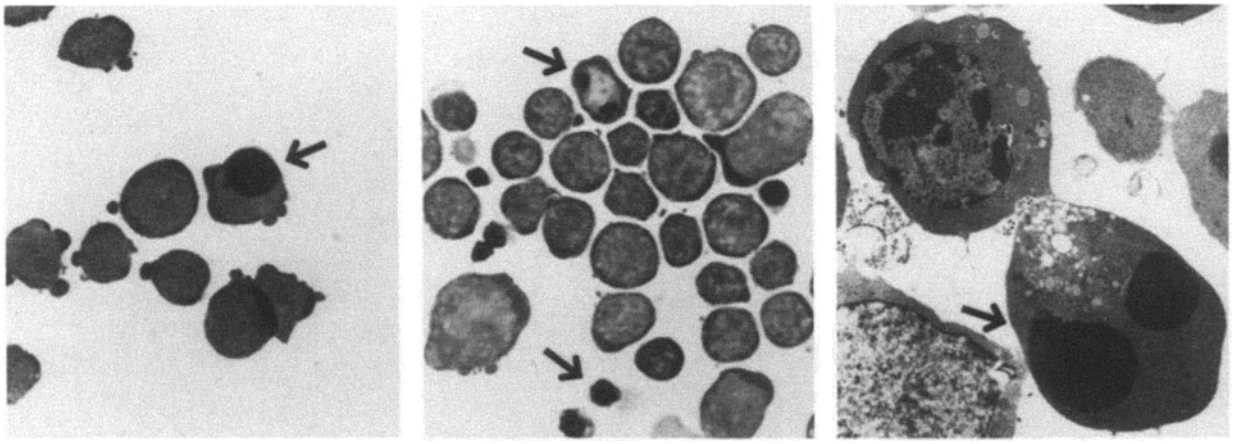

*Figure 2.* Microscopic examination of dex- and 8-br-cAMP-treated W7.2 cells reveal an apoptotic morphology. Wright-Giemsa staining was done on W7.2 cells treated with dex for 12 h (*A*) or 8-br-cAMP for 72 h (*B*). A sample of the same cells used in *B* was examined by electron microscopy (*C*). Condensed chromatin (*A*, *B*, and *C*) and apoptotic bodies (*B*) characteristic of apoptosis are indicated by the arrows shown in each photo.

nated as Apt⁻ mutants to denote a dex$^r$ phenotype due to mutations in non-GR loci.

### *Frequency of the Apt⁻ Phenotype Increases with GR Gene Copy Number*

Characterization of the 90 dex$^r$ mutants derived from W7.2 yielded only three cell lines that fit the criteria for the Apt⁻ phenotype (Table II). We reasoned that mutagenesis of W7.2 cells containing integrated copies of GR cDNA should decrease the isolation of GR-deficient mutants since GR gene copy number was elevated. WG3 and WG5 are two cell lines that were constructed by stable transfection of W7.2 with pRGRNeo. Both of these dex-sensitive cell lines contain increased levels of dex-binding activity relative to W7.2 cells (Table I), express GR cDNA specific transcripts, and have increased levels of GR transcriptional regulatory activity (data not shown).

EMS mutagenesis of WG3 and WG5 resulted in the isolation of 22 and 101 additional dex$^r$ mutants, respectively. A summary of the results from mutagenesis studies using W7.2, WG3, and WG5 is shown in Table II. Although ~10-fold fewer dex$^r$ cell lines were isolated from mutagenized WG3 and WG5 cells as compared to W7.2, a large percentage of these mutants expressed high levels of functional GR and was found to have the Apt⁻ phenotype. As shown in Table II, over 95% of WG5 mutants had an Apt⁻ phenotype as compared to <5% of W7.2 mutants. The use of WG3 and WG5 cells for mutagenesis enabled us to isolate over 60 additional dex$^r$ cell lines that contained wild-type levels of GR and were apoptosis defective (Apt⁻).

### *Apt⁻ Mutants Are Cross-resistant to Diverse Inducers of Thymocyte Apoptosis*

The ability of Bcl-2 to block cell death induced by many types of signals suggests that although independent signaling pathways can trigger apoptosis, at least some later event must be shared. To determine whether the Apt⁻ mutations affected GR-specific or shared events, dex$^r$ Apt⁻ cell lines were tested for cross resistance to other inducers of apoptosis.

Although 8-bromo-cyclic AMP (8-br-cAMP) is a more effective inducer of cell death in W7.2 cells than other cAMP analogs, its effect is delayed when compared to dex treatment (Figs. 1 and 3). Since it was unclear whether 8-br-cAMP-treated cells produced a classic apoptotic response, a morphological study was done. Fig. 2 compares the morphology of Wright-Giemsa–stained W7.2 cells exposed to dex or 8-br-cAMP. Apoptotic W7.2 cells are evident within 12 h of dex treatment (Fig. 2 *A*) as illustrated by nuclear condensation and margination (see arrow). Treatment of W7.2 cells with 8-br-cAMP resulted in a similar morphology; both condensed and marginated nuclei, as well as apoptotic bodies, were present (Fig. 2 *B*, see arrows). Moreover, nuclear condensation (see arrow), as revealed by electron microscopic examination, confirmed that 8-br-cAMP–treated W7.2 cells underwent a characteristic apoptotic cell death (Fig. 2 *C*).

Fig. 3 compares the growth of W7.2 cells and mutants after treatment with 8-br-cAMP or gamma irradiation. Consistent with the morphological evidence, 8-br-cAMP treatment of W7.2 cells resulted in a 24-h period of normal growth followed by a complete loss of W7.2 viability. In contrast, all the Apt⁻ mutants retained viability in the presence of 8-br-cAMP, while both Apt4.8 and Apt4.19 cells continued to grow normally. Although the growth of Apt3.8 and Apt5.8 was slowed after 48 h of treatment, culture viability of all the Apt⁻ mutants shown in Fig. 3 could be maintained for several passages in the presence of 8-br-cAMP (data not shown). This data clearly illustrated that these Apt⁻ cells were cross resistant to 8-br-cAMP and dex. As a positive control for a resistant phenotype, the response of Hbl2 cells to 8-br-cAMP was tested and was similar to that of Apt4.8.

Exposure to a low dose of gamma irradiation resulted in a rapid loss of viability in W7.2 cells. In comparison, Apt3.8, Apt4.8, Apt4.19, and Apt5.8 cells retained viability but were growth arrested after an identical irradiation treatment. The growth response and viability of gamma irradiated Hbl2 resembled that of the Apt⁻ mutants. The response of these

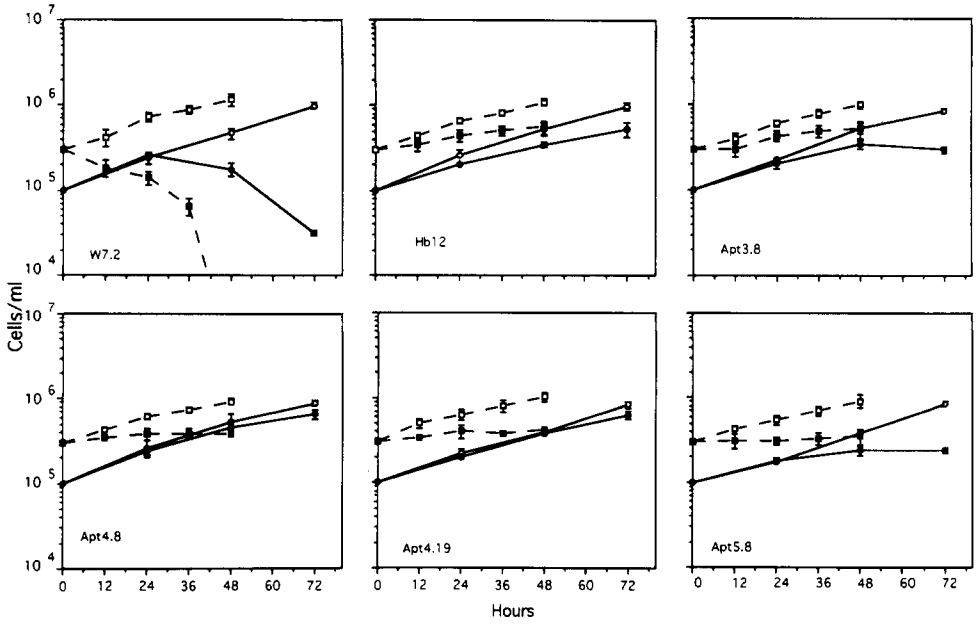


*Figure 3.* Sensitivity of W7.2, Hbl2, Apt3.8, Apt4.8, Apt4.19, and Apt5.8 cells to 8-br-cAMP or gamma irradiation. Cells were grown as described in Fig. 1 except treated with 200 μM 8-br-cAMP (*solid lines*) or 500 rads ionizing radiation (*dashed lines*). The open symbols are untreated cells and the closed symbols are treated cells.

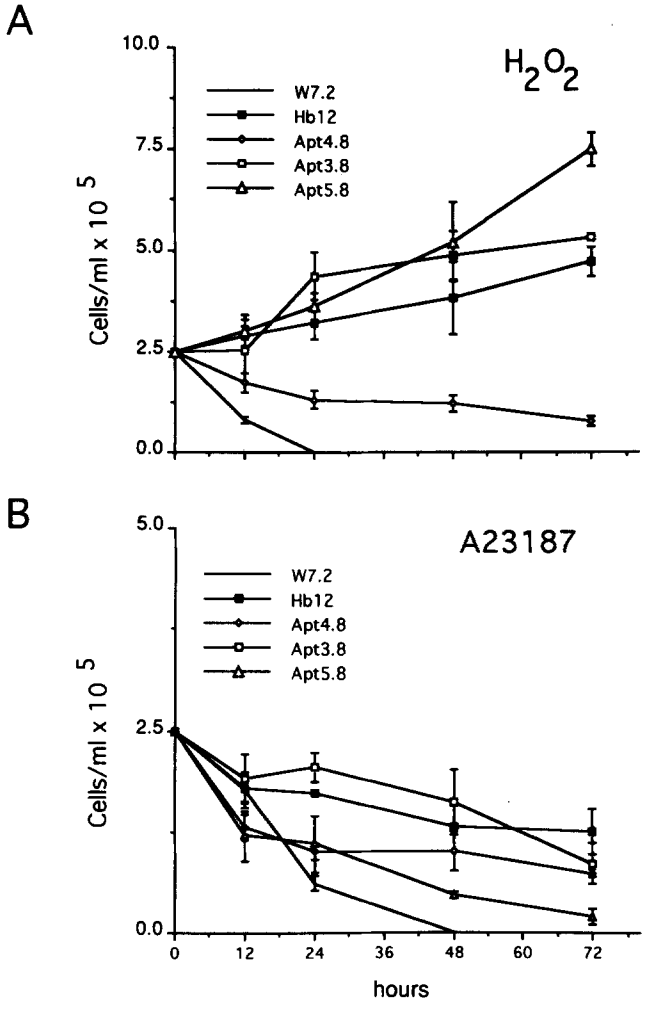


*Figure 4.* Sensitivity of W7.2, Hbl2, Apt3.8, Apt4.8, and Apt5.8 to $H_2O_2$ and calcium ionophore A23187. Cells were grown as described in Fig. 1 except in the presence of either 100 μM $H_2O_2$ (*A*) or 1.5 μM A23187 (*B*).

cells illustrates a distinction between two biological responses to gamma irradiation, growth arrest, a p53-mediated response (37), and the induction of apoptosis. In the Apt⁻ mutants, gamma irradiation–induced growth arrest appears to be unimpaired, while the mechanism controlling apoptosis induction is defective. The lack of cell death in the mutants after gamma irradiation allowed resumption of normal growth rate within a week (data not shown), while similarly treated cultures of W7.2 lost viability within 72 h (Fig. 3).

Free radical production has been implicated as a causal agent of apoptosis in response to gamma irradiation, and direct production of free radicals by $H_2O_2$ treatment causes apoptosis (12, 31). Fig. 4 *A* shows that 100 μM $H_2O_2$ caused W7.2 cells to die within 24 h of exposure. Similar treatment of the Apt⁻ cell lines revealed that while Apt4.8 cells were $H_2O_2$-sensitive, as evidenced by increased cell death and a steady decrease in cell viability, Apt3.8 and Apt5.8 cells were resistant and continued to proliferate. Although Bcl-2 protected Hbl2 cells against $H_2O_2$-induced cell death, the growth of these cells was slowed relative to Apt3.8 and Apt5.8. Together, our results indicate that $H_2O_2$ treatment mimics intracellular changes that occur before apoptotic commitment.

Intracellular calcium mobilization has been proposed to be an important step in thymocyte apoptosis (44, 48) and some studies suggest that oxidative stress may be a factor that modulates the magnitude of calcium fluxes (51, 60). Treatment of W7.2 with the calcium ionophore A23187 (A23187) has been shown to induce cell death similar to that produced by dex (46). As shown in Fig. 4 *B*, 1.5 μM A23187 rapidly induced cell death in W7.2. The same treatment also killed Apt4.8, Apt3.8, Apt5.8, and Hbl2 cells. Although Hbl2 and Apt⁻ cells were less sensitive to A23187 than W7.2, there was a prolonged, steady decline of viable cells, followed by a complete loss of viability within 7 d (data not shown). These data show that the lethal effects of A23187 bypass the blocks imposed by Apt⁻ mutations and Bcl-2.

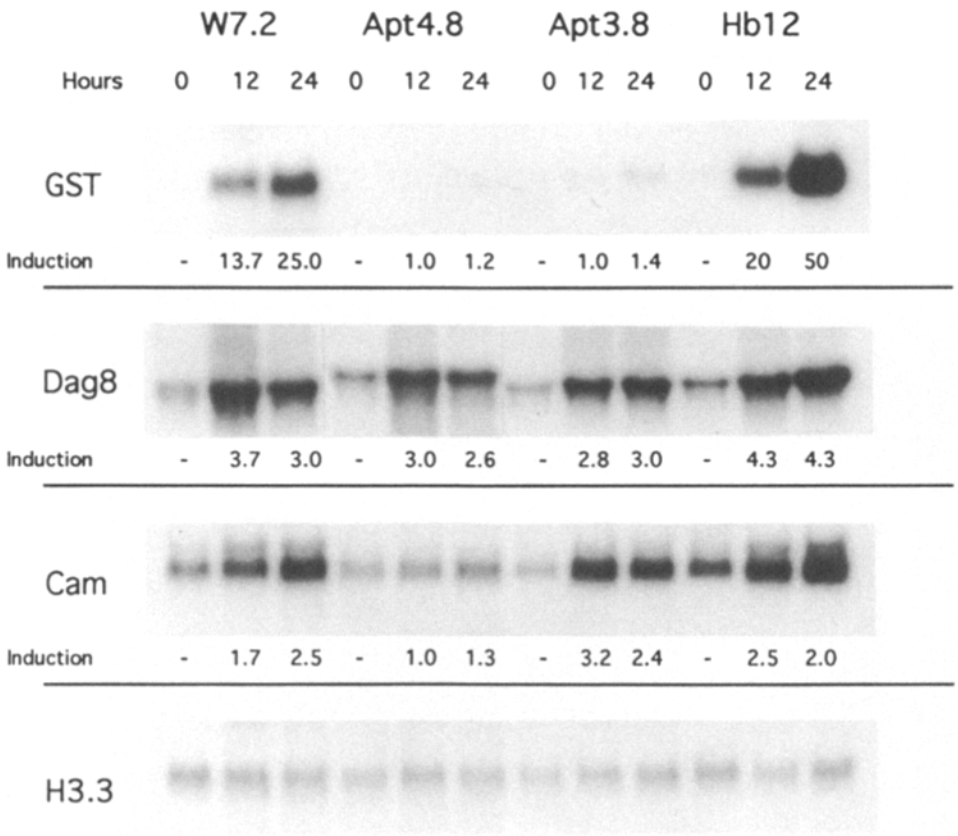


*Figure 5.* Analysis of gene expression in response to dex treatment of W7.2, Hb12, Apt3.8, and Apt4.8 cells. Northern analysis of 15 $\mu$g total RNA probed with glutathione *S*-transferase (GST), Dag-8, calmodulin (Cam), or histone (H3.3) probes. Identical RNA samples were separated on formaldehyde gels and transferred to Duralon membranes (Stratagene, La Jolla, CA). The resulting blots were hybridized with the indicated probes, quantitated, stripped, and reprobed with histone H3.3 to control for loading differences. Quantitation of transcript levels (normalized to H3.3) was done and induction values are shown relative to the signal at the zero time point.

### *Gene Expression Patterns in Dex-treated Apt⁻ and Hb12 Cells Differ*

Mutations that affect early steps of the apoptotic pathway could alter the expression pattern of gene transcripts that are normally upregulated in dex-treated W7.2 cells. In addition, comparison of dex-induced gene expression pattern of individual Apt⁻ cells with Hb12, might allow placement of the Apt⁻ blocks relative to the step affected by Bcl-2. To test these possibilities, the expression patterns of glutathione-S-transferase (GST) (23), calmodulin (Cam) (5, 20), and Dag-8 (Flomerfelt, F. A., and R. L. Miesfeld, manuscript in preparation) were examined in several Apt⁻ mutants. Although the role of GST and Cam in thymocyte apoptosis is unknown, their elevated expression in preapoptotic W7.2 cells may be indicative of cell death–associated changes in redox and calcium homeostasis, respectively (20, 23). Dag-8 was isolated by subtraction hybridization from dex-treated W7.2 cells, and its function is also unknown (Flomerfelt, F. A., and R. L. Miesfeld, manuscript in preparation.)

Fig. 5 shows the results of Northern analysis of RNA obtained from W7.2, Apt3.8, Apt4.8, and Hb12 cells exposed to dex for 0, 12, and 24 h. Mouse histone H3.3 RNA levels were measured as an internal control. GST expression increased rapidly in both W7.2 and Hb12 cells, but no changes in basal GST transcript levels were observed in Apt4.8 or Apt3.8 cells. Identical results were found in 10 other Apt⁻ cell lines including Apt5.8 (data not shown). Dag-8 RNA levels increased uniformly in W7.2, Hb12, Apt4.8, and Apt3.8 cells after dex treatment. This finding is consistent with Dag-8 being a dex-regulated GR target gene (either primary or secondary) rather than a gene that responds to cellular changes associated with apoptosis. Cam message was induced in dex-treated W7.2 as expected (5, 20). Interestingly, a similar induction of Cam transcripts was also seen in response to dex in both Apt3.8 and Hb12 cells. In contrast, no change was observed in Cam RNA levels of most Apt⁻ cell lines including Apt4.8 and Apt5.8 (data not shown). The CAM expression data suggested that Apt4.8 and Apt3.8 contain mutations that affect distinct pathway steps.

### *Heterokaryon Fusions Reveal Multiple Apt⁻ Complementation Groups*

Although it is not possible to perform standard genetic crosses with somatic cells, it is feasible to test for phenotypic complementation using cell fusion studies. Since stable synkaryon fusion cell lines may contain incomplete sets of genomic material due to chromosome loss (6), a rapid transient heterokaryon complementation assay was developed that is similar to that previously used by others (4, 7, 66). This procedure entailed the production of doubly labeled, fluorescent heterokaryons by polyethylene glycol (PEG) fusion, purification of heterokaryons using fluorescent-activated cell sorting (FACS), and determining the effects of dex on nondividing heterokaryon populations.

Fig. 6 *A* shows the FACS analysis of a typical heterokaryon purification in which the sorted cell population was 96.4% double positive for fluorescein and rhodamine labels. Forward- and side-scatter analysis showed that the purified, double-labeled heterokaryons were viable and larger than nonfused cells (data not shown). Fig. 6 *B* shows micrographs of fluorescent unsorted- and sorted-fused cells. Fused cells contained only 0.2% double-labeled cells (see arrow in the

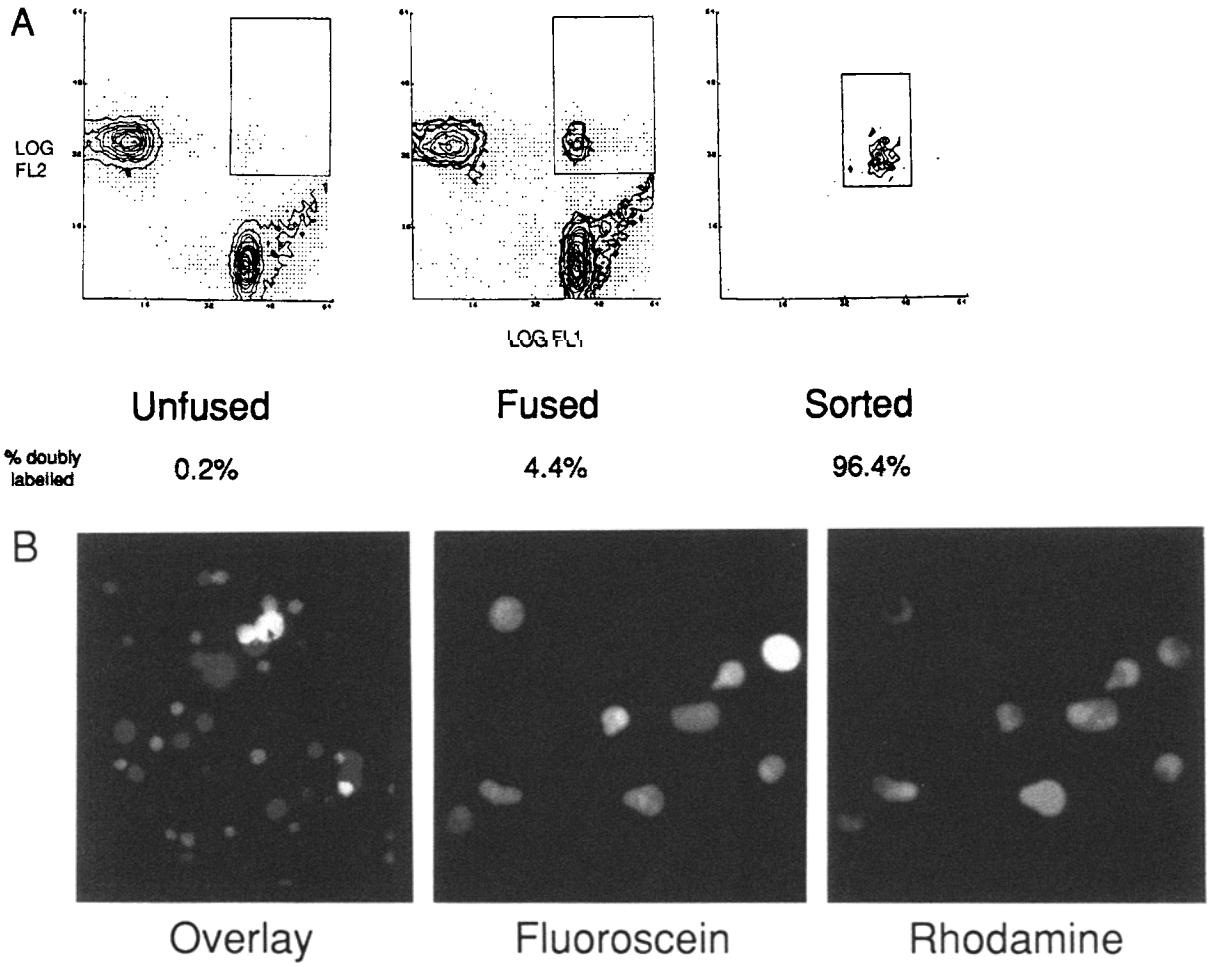


*Figure 6.* Production and purification of double-labeled heterokaryons. (*A*) FACS analysis of fusion procedure plotted as log fluorescence rhodamine (*FL2*) vs log fluorescence fluorescein (*FL1*) for nonfused and fused, sorted cell populations. The percentage of double-labeled cells was determined by the proportion of cells found within the box as shown. (*B*) Microscopic examination of fused cell populations using false color imaging. Cells shown by arrow represent the minority of double-positive heterokaryons in an unsorted-fused population. After FACS purification, most sorted cells are double labeled as seen in the two panels labeled fluorescein and rhodamine that show a single field of cells.

left panel of Fig. 6 *B*), but after FACS purification, most cells were double labeled and greater than 95% of the heterokaryons contained just two nuclei. Sorted heterokaryons were divided into two equal populations in media containing 1% calf serum to retard cell division. Dex was added to one of these samples, and after five days, dex sensitivity was assayed by determining cell viability. A heterokaryon population was considered to be dex sensitive if the number of viable, dex-treated cells was less than 10% the number of untreated viable cells after 5 d. Photomicrographs, shown in Fig. 7 *A*, demonstrate that control homokaryon fusions of Apt3.2 and Apt4.8 are dex$^r$ and retain viability, whereas Apt3.2 × Apt4.8 heterokaryons are dex sensitive (Fig. 7 *B*). These results led to the following conclusions: (*a*) that Apt4.8 contains sufficient levels of functional GR to induce apoptosis when fused to a GR-deficient cell line (i.e., Apt3.2), (*b*) that the mutation in Apt4.8 is recessive, and (*c*) that this assay provided a method to functionally test GR in recessive Apt$^-$ mutants.

To determine whether the fusion assay could be used to detect dominant mutations, Hb12 and several Apt$^-$ cell lines were fused to W7.2. As shown in Table III, the mutations in Apt3.2, Apt3.8, Apt4.8, and Apt4.19 were recessive when fused to W7.2. Fusions with additional Apt$^-$ cell lines (data not shown) failed to identify any dominant mutants. Importantly, the dex$^r$ phenotype of Hb12 cells was dominant in the heterokaryon fusion assay, as expected based on the dominant activity of Bcl-2.

Fig. 8 summarizes the results of complementation assays of eight different Apt$^-$ mutants. The grid scores (dex sensitive; yes or no) are the result of at least three separate experiments using more than $5 \times 10^4$ viable heterokaryons that were greater than 85% double labeled. Each of the mutant cell lines was first fused with Apt3.2 (group *A*, GR defective) to functionally test for GR mutations. Mutants that complemented Apt3.2 were then tested in paired combinations. As shown in Fig. 8, heterokaryons produced by fusing Apt4.8 and Apt3.8 were dex sensitive. This data functionally demonstrated that these cell lines define different, non-GR complementation groups (groups *B* and *C*). Likewise, fusions of Apt5.8 to either Apt3.8 or Apt4.8 defined a third non-GR complementation group (group *D*). Two additional

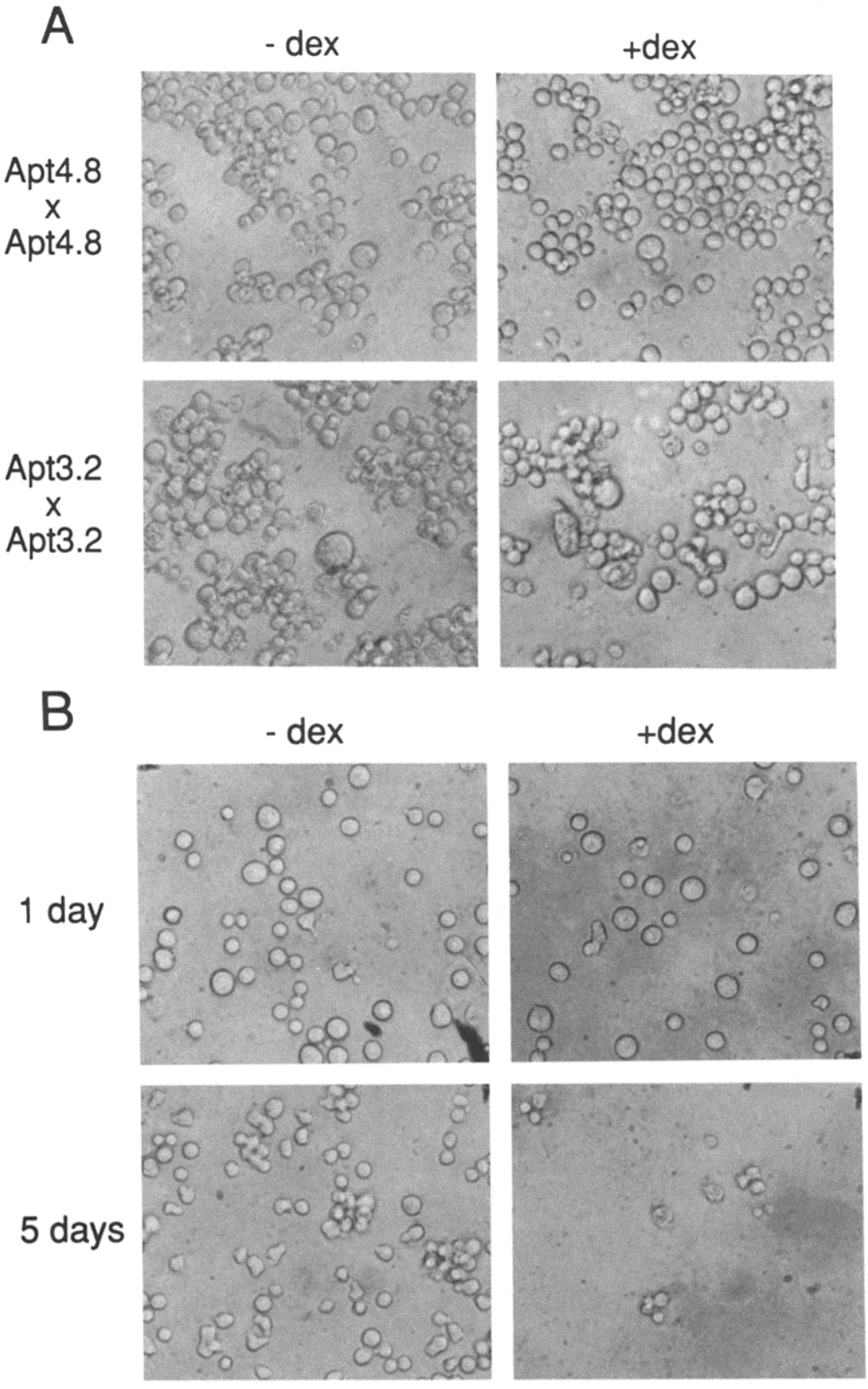


*Figure 7.* Transient heterokaryon assays detect complementation between Apt4.8 ($GR^+$) and GR-defective Apt-3.2 cells. Differentially labeled cells were fused and homokaryons (*A*) or heterokaryons (*B*) were purified and analyzed by phase microscopy. Dex-treated homokaryons of either Apt4.8 or Apt3.2 retained viability in the presence or absence of dex for 5 d (*A*). Heterokaryons produced by fusion between Apt3.2 and Apt4.8 underwent dex-dependent cell death within 5 d (*B*).

non-GR complementation groups, represented by the WG5-derived $Apt^-$ mutants, Apt5.45 (group *E*) and Apt5.60 (group *F*), were also identified with this assay. Importantly, none of the cell lines tested belong to more than one complementation group suggesting that multiple apoptotic mutations in our panel of $Apt^-$ cell lines may be rare. Group C, which contains the most members includes Apt4.8, Apt4.19, and two WG5-derived cell lines, Apt5.100 and Apt5.26.

*Table III. Apt⁻ Mutations Are Recessive in Fusions with W7.2*

| Fusion | Cell line | Dex sensitive |
|---|---|---|
| 1 | Apt3.2 × W7.2 | yes |
| 2 | Apt4.8 × W7.2 | yes |
| 3 | Apt3.8 × W7.2 | yes |
| 4 | Apt4.19 × W7.2 | yes |
| 5 | Hb12 × W7.2 | no |

Criterion for dex sensitivity was done as described in Fig. 8.

These group C Apt⁻ mutants cannot be siblings since each was clonally isolated from independent mutagenesis experiments.

## Discussion

### *Diverse Apoptotic Signals Use A Common Pathway*

In vertebrates, many types of signals can trigger apoptosis to remove unwanted or potentially harmful cells. Since various apoptotic signals (e.g., glucocorticoids and gamma irradiation) use specific, non-overlapping signal transduction pathways, they must converge on a set of common events that cause cell death. Events that comprise the common apoptotic pathway are functionally distinct from those that are required for transmission of a particular signal. For example, defects in the common apoptotic pathway should block apoptosis induced by many different signals, while mutations in signal pathways should only block apoptosis induced by a particular signal. What are the molecular characteristics of the pathway that coordinates diverse signals and initiates cell death when appropriate? It is possible that individual signal pathways converge at a common step that directly determines apoptotic commitment. Alternatively, diverse signal pathways may converge upstream of the final commitment point. In this case, apoptotic signals would lead to a shared set of events that precede the commitment step.

To date, the only genetic evidence for a common apoptotic pathway in vertebrates has been supplied by genes, like Bcl-2, that dominantly provide cross resistance to a number of apoptosis inducers (31, 63, 67). This data suggests that although apoptosis can be induced by signal-specific pathways, Bcl-2 defines a later, shared event. However, information regarding additional common precommitment events in the apoptotic pathway has been lacking. We have isolated a number of recessive mutants that are cross-resistant to dex, 8-br-cAMP, and gamma irradiation (Table IV). These mutant phenotypes contrast with previously identified mutants that block a signal- or tissue-specific pathway. For example, p53 appears to be essential for irradiation-induced thymocyte apoptosis (41) while the transcription factor, nur77, seems to be required for TCR-mediated cell death (40, 68). Functional disruption of either p53 or nur77 does not affect glucocorticoid-induced apoptosis in thymocytes, a pathway that absolutely requires GR (17). Conversely, the GR deficiency in Apt3.2 cells did not block apoptotic induction by gamma irradiation or 8-br-cAMP (data not shown). Therefore, the observed cross resistance of the Apt⁻ mutants indicates that these cells contain mutations in specific gene products that are required after the point of signal convergence in the apoptotic pathway.

### *The Common Apoptotic Pathway Contains Separate Events*

Currently, the only step that has been identified as part of a common apoptotic pathway is defined by Bcl-2. Characterization of the Apt⁻ mutants and Hb12 identified several phenotypic groups, based on differences in gene expression (Fig. 5) and cross resistance (Table IV), that were suggestive of additional common apoptotic pathway steps. In particular, the differential sensitivity to $H_2O_2$ of Apt4.8 and Apt3.8 cells, coupled with the finding that dex-dependent Cam gene expression was upregulated in Apt3.8, but not Apt4.8, indicated that Apt3.8 and Apt4.8 have mutations in separate genetic loci. Furthermore, although Apt⁻ and Hb12 cell lines shared common features of cross resistance, only Hb12 cells responded to dex treatment by an increase in GST transcript levels. To functionally test whether Apt3.8 and Apt4.8 represent separate complementation groups, and to determine whether the chemically induced Apt⁻ mutations were dominant or recessive, a rapid transient heterokaryon complementation assay was used.

Results from the heterokaryon assay provided three insights into the Apt⁻ phenotype: (*a*) Apt⁻ cells contain sufficient GR to produce dex-sensitive heterokaryons when fused with Apt3.2; (*b*) the Apt⁻ mutations were recessive in fusions with W7.2 cells; and (*c*) the recessive mutations that block apoptosis in the Apt⁻ cells tested define five non-GR complementation groups. Phenotypic differences in Apt4.8,

| | A | B | C | C | C | C | D | E | F |
|---|---|---|---|---|---|---|---|---|---|
| | Apt3.2 | | | | | | | | |
| A | Apt3.2 | no | Apt3.8 | | | | | | |
| B | Apt3.8 | yes | no | Apt4.8 | | | | | |
| C | Apt4.8 | yes | yes | no | Apt4.19 | | | | |
| C | Apt4.19 | yes | yes | no | no | Apt5.26 | | | |
| C | Apt5.26 | yes | yes | no | no | no | Apt5.100 | | |
| C | Apt5.100 | yes | yes | no | no | no | no | Apt5.8 | |
| D | Apt5.8 | yes | yes | yes | yes | n.d. | n.d. | no | Apt5.45 |
| E | Apt5.45 | yes | yes | yes | n.d | n.d. | n.d. | yes | n.d. |
| F | Apt5.60 | yes | yes | yes | n.d. | n.d. | n.d. | yes | yes |

*Figure 8.* Summary of heterokaryon fusion assays. Each grid represents the results of at least three separate fusion experiments. Positive complementation was scored when the number of cells in the dex-treated sample was less than 10% that of the untreated sample at the end of a 5-d period. Uppercase letters represent the tentative assignment of complementation groups (*n.d.*, not done).

*Table IV. Summary of Cross-resistance of W7.2, Hb12, Cell Lines to Various Inducers of Apoptosis*

| Apoptotic inducer | Cell line | | | | |
|---|---|---|---|---|---|
| | W7.2 (wild-type) | Hb12 (Bcl-2+) | Apt3.8 (Group B) | Apt4.8 (Group C) | Apt5.8 (Group D) |
| dex | − | ++ | ++ | +++ | +++ |
| 8-br-cAMP | − | ++ | ++ | +++ | ++ |
| g-irradiation | − | ++ | ++ | ++ | ++ |
| $H_2O_2$ | − | ++ | ++ | + | +++ |
| A23187 | − | +/− | +/− | +/− | +/− |

Scoring was based on the growth curves shown in Figs. 2 *B*, 3, and 4 as follows: − denotes lack of resistance (fully sensitive); + denotes partial resistance; ++ denotes resistant and slowed growth; +++ denotes fully resistant with near normal growth.

Apt3.8, and Apt5.8 (see Table IV) supported the assignation of these three cell lines to three different complementation groups. This data suggests that the mutations in Apt4.8, Apt3.8, and Apt5.8 define separate components of the common apoptotic pathway in W7.2 cells that depend on active gene expression. Furthermore, our data excludes the possibility that apoptosis is blocked in these Apt$^-$ cell lines by dominant negative mutations or by dominantly acting proteins like Bcl-2. Complementation group C contained 50% (4/8) of the Apt$^-$ mutants analyzed by the fusion assay and each of these cell lines was derived from independent mutagenesis experiments. One interpretation of the high recovery of group C mutant alleles is that few genes are involved in the precommitment pathway. Alternatively, it is possible that the group C determinant is highly sensitive to mutagenesis or that group C mutants may be heterozygous for a defect in a rate-limiting gene required to induce apoptosis, similar to the preponderance of GR-defective dex$^r$ mutants in W7.2 and S49 cells ([16, 24] and Table II). However, since backcrossing and *cis-trans* tests are not possible with this system, the genetic interpretations of these data are somewhat limited.

### *A Model for Apoptotic Pathway Transit*

Our investigation of the apoptotic pathway in murine thymocytes has led to the functional identification of multiple events, defined by recessive mutations, that are required for apoptosis induction and are distinct from a later event that can be antagonized by Bcl-2. Fig. 9 shows a schematic model in which signal pathways initiated by dex, 8-br-cAMP, and gamma irradiation converge upstream of the Apt$^-$ mutations to initiate a common apoptotic pathway. In addition, some pathway steps can be bypassed by either $H_2O_2$ or calcium ionophore A23187 treatment. The differences in gene expression patterns between dex-treated W7.2, Apt3.8, Apt4.8, and Hb12 indicate that apoptotic pathway transit may trigger an interdependent cascade of gene expression. The recessive mutation in Apt4.8 cells, which provides cross resistance to dex, 8-br-cAMP, and gamma irradiation, is bypassed by $H_2O_2$ treatment (see Table IV). This data indicates that the gene mutated in Apt4.8 must be expressed in W7.2 cells to undergo apoptosis in response to dex, 8-br-cAMP, and gamma irradiation but not to $H_2O_2$. This idea is consistent with previous studies that have shown a requirement for intact transcriptional regulatory domains of GR (17), p53 (41, 71), *c-myc* (21), and nur77 (68) to induce apoptosis.

Since Apt4.8 (group C) is $H_2O_2$-sensitive, and antioxidants block apoptosis (31), $H_2O_2$ treatment appears to mimic intracellular changes that occur in a precommitment step to promote apoptosis. However, oxidative stress, produced by $H_2O_2$ treatment, is not sufficient to induce apoptosis in Apt3.8 and Apt5.8 cells (Fig. 4). One interpretation of this data is that gene products, missing or reduced in Apt3.8 and Apt5.8 cells, respond to increased oxidative stress, and promote induction of apoptosis under this condition. Finally, since A23187 treatment was lethal to all the Apt$^-$ mutants and Hb12, changes in calcium localization appear to be a later step. A minimum threshold signal strength to overcome pathway barriers (represented by *dashed lines* in Fig. 9) is indicated since lower concentrations of $H_2O_2$ and A23187

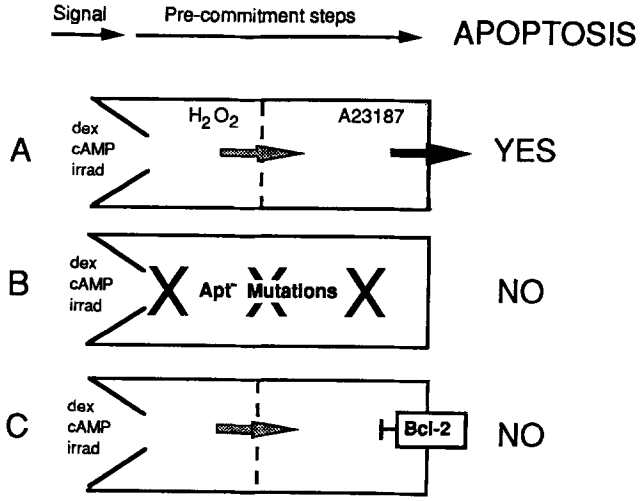


*Figure 9.* A model for dex-induced apoptosis in W7.2 cells. This model proposes that dex-induced apoptosis results from transit through a defined genetic pathway that requires regulated gene expression. The temporal sequence of events is (*1*) reception and transmission of the apoptotic signal; (*2*) transcriptional regulation and threshold expression of specific genes; (*3*) changes in cellular homeostasis and specific gene product levels that meet conditions required for transit through a precommitment period that may be positively or negatively affected by additional factors; and (*4*) commitment to undergo apoptosis followed by activation of effectors that bring about apoptotic cell death. In this model, accumulation of reactive oxygen species and calcium mobilization are involved at different steps. Apt$^-$ mutations block passage through early steps of the pathway, illustrated by crosses, while Bcl-2 blocks apoptosis by antagonizing a later step.

(data not shown), as well as reduced GR content (Tables I and II), are insufficient to induce apoptosis.

This model proposes that commitment to undergo apoptotic cell death occurs when all the conditions required to induce apoptosis have been met (Fig. 9 *A*). Our results suggest that the recessive, Apt⁻ mutations block transit through the precommitment phase (Fig. 9 *B*). We predict that the Apt⁻ mutations affect genes that are specifically required for apoptosis. More specifically, based on the $H_2O_2$ sensitivity of Apt4.8 compared to that of Apt5.8 and Apt3.8, we propose that the mutation in Apt4.8 affects an early pathway step. Furthermore, our data suggests that the Apt3.8 mutation, which confers cross resistance to dex, gamma irradiation, 8-br-cAMP, and $H_2O_2$, affects a later event, before the step affected by Bcl-2. Based on the dex-dependent GST and Cam gene expression patterns of Hbl2 cells, we suggest that Bcl-2 antagonizes a relatively late step that may define an irreversible commitment point (Fig. 9 *C*). This data contrasts with recent reports that imply that Bcl-2 may block apoptosis by preventing oxidative damage (31, 34) or by blocking calcium mobilization to the cytoplasm (39). However, it is not clear whether these are primary effects of Bcl-2 expression (31), or whether these effects are due to normal repair and homeostatic mechanisms that remain active in non-apoptotic cells.

The striking observation that Bcl-2 protects against such a wide variety of apoptotic inducers also supports the notion that the dominant activity of Bcl-2 functions downstream of putative effector molecules (32). Since all of the Apt⁻ cell lines we tested were cross-resistant to dex, 8-br-cAMP, and gamma irradiation, we suggest that multiple common precommitment steps, which may provide a mechanism to coordinate regulatory inputs (i.e., cell death checkpoints), are used by diverse apoptotic signals. This idea could be extended to propose that Apt⁻ mutations define shared steps in a common pathway, rather than identifying individual components of multiple parallel pathways. However, distinguishing between shared and parallel pathways will require more information of the genes defined by the Apt⁻ mutations.

### *A Genetic Model of Vertebrate Apoptosis*

One of the major goals of this work was to provide a cell culture model to further investigate the induction of apoptosis in a vertebrate system. Although *C. elegans* provided a good invertebrate system, differences in its cell death program when compared to vertebrate apoptosis, and the inability to carry out detailed biochemical studies, limit its usefulness. To address this problem, W7.2 cells were used to generate a panel of apoptosis-defective mutants that provided a genetic system to study thymocyte apoptosis.

Phenotypic characterization of the Apt⁻ cell lines indicates that they contain mutations that block apoptosis in response to a variety of signals. Although the identity and function of the mutated genes are unknown, our studies indicate that they define a previously unknown group of cell death genes with novel characteristics. The Apt⁻ cells provide the first example of recessive mutations in vertebrates that result in cross resistance to multiple apoptotic inducers. This finding functionally distinguishes the recessive W7.2 Apt⁻ mutants from cell lines that express genes like *Bcl-2* that dominantly suppress cell death (see Table III, and [58]). Furthermore, it is unlikely that any Apt⁻ mutants contain loss of function mutations in Bax, a protein that binds to and inactivates Bcl-2 (49), since W7.2 cells contain negligible levels of Bcl-2 protein and none of the Apt⁻ mutants exhibited a dex-dependent increase in GST transcripts characteristic of Bcl-2-protected Hbl2 cells (Fig. 5).

Some putative vertebrate cell death genes can induce apoptosis through dysregulated expression. Two such examples are the multifunctional *c-myc* protein, that under special conditions can promote cell death (43), and the recently described protease, interleukin-1$\beta$-converting enzyme (ICE), which has homology to ced3 (45, 72). At this point, however, it has been difficult to discern cause from effect since ectopic expression of these proteins may result in aberrant cellular conditions that create apoptotic signals by default. For example, overexpression of the murine ced3 homologue, ICE, can induce apoptosis in RAT-1 cells (45). However, no ICE transcripts were detected by Northern analysis of W7.2 cells treated with dex for 0, 6, 12, or 24 h using a full-length ICE cDNA probe (Flomerfelt, F. A., and R. L. Miesfeld, unpublished data). This finding underscores the problem in differentiating between gene products that can produce an apoptotic signal in certain cases, from those that are required to promote apoptosis. The Apt⁻ mutants provide a system that should resolve some of these problems.

A cell line system, such as W7.2, permits detailed biochemical analysis and facilitates the use of molecular techniques that can be used to further study apoptosis. For example, biochemical characterization of W7.2 and Apt⁻ mutants can be done to quantify the role of changes in reactive oxygen levels and calcium mobilization in apoptosis. Additionally, the Apt⁻ cells may also provide a useful format to test drug-induced therapeutic induction of apoptosis. Strategies to functionally clone genomic DNA by complementation of individual Apt⁻ mutant cell lines may be possible since W7.2 cells require 18–24 h of dex treatment to commit a population to undergo apoptosis (19). For instance, FACS purification, or Ara C selection, could be used within this period to isolate transfected cells that undergo dex-dependent growth arrest. The goal of this approach, and other strategies under consideration, would be to rescue transfected mutants that regain hormone-dependent induction of apoptosis. Finally, the Apt⁻ mutants offer a method to systematically evaluate the role of genes in apoptosis that have been cloned by virtue of their differential expression in apoptotic cells (5, 25, 27, 53).

The authors would like to thank Barbara Corolis for her devotion to this project and expertise with the FACS machine, Ron Lynch for expert help with microscopy and image analysis, Debra Gordon for helpful discussion and encouragement throughout, David Gailbraith for advice and expertise in designing the double-labeling heterokaryon cell fusion assay, and Claire Payne for providing the electron micrograph. We also thank Bernard Futscher for providing the histone H3.3 gene primers, Dr. David D. Chaplin for generously providing the murine ICE cDNA, and Anna Collins for manuscript preparation. Members of our lab, David Askew, Nancy Chamberlain, Mark Chapman, and Debra Gordon are also acknowledged for their insightful comments.

This work was supported by a National Institutes of Health grant (GM40738) to R. L. Miesfeld and by a generous donation from the Jack Doyle Memorial Fund. R. L. Miesfeld is a Scholar of the Leukemia Society of America.

Received for publication 19 May 1994 and in revised form 12 August 1994.

*References*


1. Arends, M. J., R. G. Morris, and A. H. Wyllie. 1990. Apoptosis: the role of the endonuclease. *Am. J. Pathol.* 136:593–608.
2. Ausubel, F., R. Brent, R. Kingston, D. Moore, J. G. Seidman, J. M. Smith, and K. Struhl. 1989. *In* Current Protocols in Molecular Biology. Green Publishing Co. John Wiley and Sons, New York. pp. 4.9.2–4.9.8.
3. Bansal, N., A. Houle, and G. Melnykovych. 1991. Apoptosis: mode of cell death induced in T cell leukemia lines by dexamethasone and other agents. *(FASEB (Fed. Am. Soc. Exp. Biol.) J.* 5:211–216.
4. Baron, M. H., and T. Maniatis. 1986. Rapid reprogramming of globin gene expression in transient heterokaryons. *Cell.* 46:591–602.
5. Baughman, G., M. T. Harrigan, N. F. Campbell, S. J. Nurrish, and S. Bourgeois. 1991. Genes newly identified as regulated by glucocorticoids in murine thymocytes. *Mol. Endocrinol.* 5:637–644.
6. Blau, H. M. 1989. How fixed is the differentiated state? Lessons from heterokaryons. *Trends Genet.* 5:268–272.
7. Blau, H. M., G. K. Pavlath, E. C. Hardeman, C.-P. Chiu, L. Silberstein, S. G. Webster, S. C. Miller, and C. Webster. 1985. Plasticity of the differentiated state. *Science (Wash. DC).* 230:758–766.
8. Boobis, A. R., D. J. Fawthrop, and D. S. Davies. 1989. Mechanisms of cell death. *TIPS.* 10:275–280.
9. Bourgeois, S., and J. C. Gasson. 1985. Genetic and epigenetic bases of glucocorticoid resistance in lymphoid cell lines. *In* Biochemical Actions of Hormones. Vol. 12. G. Litwack, editor. Academic Press, New York. pp. 311–315.
10. Briehl, M. M., and R. L. Miesfeld. 1991. Isolation and characterization of transcripts induced by androgen withdrawal and apoptotic cell death in the rat ventral prostate. *Mol. Endocrinol.* 5:1381–1388.
11. Bursch, W., F. Oberhammer, and R. Schulte-Hermann. 1992. Cell death by apoptosis and its protective role against disease. *Trends Pharmacol. Sci.* 13:245–251.
12. Buttke, T. M., and P. A. Sandstrom. 1994. Oxidative stress as a mediator of apoptosis. *Immunol. Today.* 15:7–10.
13. Cleary, M. L., S. D. Smith, and J. Sklar. 1986. Cloning and structural analysis of cDNAs for *blc-2* and a hybrid *blc-2*/immunoglobulin transcript resulting from the t(14;18) translocation. *Cell.* 47:19–28.
14. Cohen, J. J. 1993. Apoptosis. *Immunol. Today.* 14:126–130.
15. Cohen, J. J., R. C. Duke, V. A. Fadok, and K. S. Sellins. 1992. Apoptosis and programmed cell death in immunity. *Annu. Rev. Immunol.* 10: 267–293.
16. Danielsen, M., D. O Peterson, and M. R. Stallcup. 1983. Immunological selection of variant mouse lymphoid cells with altered glucocorticoid responsiveness. *Mol. Cell. Biol.* 3:1310–1316.
17. Dieken, E. S., and R. L. Miesfeld. 1992. Transcriptional transactivation functions localized to the glucocorticoid receptor N terminus are necessary for steroid induction of lymphocyte apoptosis. *Mol. Cell. Biol.* 12:589–597.
18. Dieken, E. S., E. U. Meese, and R. L. Miesfeld. 1990. nt[i] glucocorticoid receptor transcripts lack sequences encoding the amino-terminal transcriptional modulatory domain. *Mol. Cell. Biol.* 10:4574–4581.
19. Dowd, D. R., and R. L. Miesfeld. 1992. Evidence that glucocorticoid- and cyclic AMP-induced apoptotic pathways in lymphocytes share distal events. *Mol. Cell. Biol.* 12:3600–3608.
20. Dowd, D. R., P. N. MacDonald, B. S. Komm, M. R. Haussler, and R. L. Miesfeld. 1991. Evidence for early induction of calmodulin gene expression in lymphocytes undergoing glucocorticoid-mediated apoptosis. *J. Biol. Chem.* 266:18423–18426.
21. Evan, G. I., A. H. Wyllie, C. S. Gilbert, T. D. Littlewood, H. Land, M. Brooks, C. M. Waters, L. Z. Penn, and D. C. Hancock. 1992. Induction of apoptosis in fibroblasts by c-myc protein. *Cell.* 69:119–128.
22. Fanidi, A., E. A. Harrington, and G. I. Evan. 1992. Cooperative interaction between *c-myc* and *blc-2* proto-oncogenes. *Nature (Lond.).* 359: 554–556.
23. Flomerfelt, F. A., M. M. Briehl, D. R. Dowd, E. S. Dieken, and R. L. Miesfeld. 1993. Elevated glutathione S-transferase gene expression is an early event during steroid-induced lymphocyte apoptosis. *J. Cell. Physiol.* 154:573–581.
24. Gehring, U. 1980. Cell genetics of glucocorticoid responsiveness. *In* Biochemical Actions of Hormones. Vol. 7. G. Litwack, editor. Academic Press, New York. pp. 205–223.
25. Goldstone, S. D., and M. F. Lavin. 1991. Isolation of a cDNA clone, encoding a human β-galactosidase binding protein, overexpressed during glucocorticoid-induced cell death. *Biochem. Biophys. Res. Commun.* 178:746–750.
26. Golstein, P., D. M. Ojcius, and D. E. Young. 1993. Cell death mechanisms and the immune system. *Immunol. Rev.* 121:29–65.
27. Harrigan, M. T., G. Baughman, N. F. Campbell, and S. Bourgeois. 1989. Isolation and characterization of glucocorticoid and cyclic AMP-induced genes in T-lymphocytes. *Mol. Cell. Biol.* 9:3438–3446.
28. Harris, A. W., A. D. Bankhurst, S. Mason, and N. L. Warner. 1973. Differentiated functions expressed by cultured mouse lymphoma cells. *J. Immunol.* 110:431–438.
29. Hickman, J. A. 1992. Apoptosis induced by anticancer drugs. *Can. Met. Rev.* 11:121–139.
30. Hockenbery, D., G. Nuñez, C. Milliman, R. D. Schreiber, and S. J. Korsmeyer. 1990. Bcl-2 is an inner mitochondrial membrane protein that blocks programmed cell death. *Nature (Lond.).* 348:334–336.
31. Hockenbery, D. M., Z. N. Oltvai, X.-M. Yin, C. L. Milliman, and S. J. Korsmeyer. 1993. Bcl-2 functions in an antioxidant pathway to prevent apoptosis. *Cell.* 75:241–251.
32. Jacobson, M. D., and G. I. Evan. 1994. Breaking the ice: structural and functional similarities have been discovered between two mammalian proteins, Bcl-2 and interleukin 1b-converting enzyme, and proteins encoded by nematode cell-death genes. *Curr. Biol.* 4:337–340.
33. Johnson, E. M., Jr., and T. L. Deckwerth. 1993. Molecular mechanisms of developmental neuronal death. *Annu. Rev. Neurosci.* 16:31–46.
34. Kane, D. J., T. A. Sarafian, R. Anton, H. Hahn, E. B. Gralla, J. S. Valentine, T. Örd, and D. E. Bredesen. 1993. Bcl-2 inhibition of neural death: decreased generation of reactive oxygen species. *Science (Wash. DC.)* 262:1274–1277.
35. Kerr, J. F. R., and B. V. Harmon. 1991. Definition and incidence of apoptosis: an historical perspective. *In* Apoptosis: The Molecular Basis of Cell Death. Cold Spring Harbor Laboratory Press, Cold Spring Harbor, NY. 5–29.
36. Koury, M. J. 1992. Programmed cell death (apoptosis) in hematopoiesis. *Exp. Hematol.* 20:391–394.
37. Kuerbitz, S. J., B. S. Plunkett, W. V. Walsh, and M. B. Kastan. 1992. Wild-type p53 is a cell cycle checkpoint determinant following irradiation. *Proc. Natl. Acad. Sci. USA.* 89:7491–7495.
38. Kyprianou, N., and J. T. Isaacs. 1988. Activation of programmed cell death in the rat ventral prostate after castration. *Endocrinology.* 122:552–562.
39. Lam, M., G. Dubyak, L. Chen, G. Nunez, R. L. Miesfeld, and C. W. Distelhorst. 1994. Evidence that BCL-2 represses apoptosis by regulating endoplasmic reticulum-associated $Ca^{2+}$ fluxes. *Proc. Natl. Acad. Sci. USA.* 91:6569–6573.
40. Liu, Z.-G., S. W. Smith, K. A. McLaughlin, L. M. Schwartz, and B. A. Osborne. 1994. Apoptotic signals delivered through the T-cell receptor of a T-cell hybrid require the immediate-early gene *nur77*. *Nature (Lond.).* 367:281–284.
41. Lowe, S. W., E. M. Schmitt, S. W. Smith, B. A. Osborne, and T. Jacks. 1993. p53 is required for radiation-induced apoptosis in mouse thymocytes. *Nature (Lond.).* 362:847–849.
42. Malorni, W., and G. Donelli. 1992. Cell death. General features and morphological aspects. *Ann. NY Acad. Sci.* 663:218–233.
43. Martin, S. J., D. R. Green, and T. G. Cotter. 1994. Dicing with death: dissecting the components of the apoptosis machinery. *TIBS (Trends Biochem. Sci.)* 1:26–30.
44. McConkey, D. J., P. Nicotera, P. Hartzell, G. Bellomo, A. H. Wyllie, and S. Orrenius. 1989. Glucocorticoids activate a suicide process in thymocytes through an elevation of cytosolic $Ca^{2+}$ concentration. *Arch. Biochem. Biophys.* 269:365–370.
45. Miura, M., H. Zhu, R. Rotello, E. A. Hartwieg, and J. Yuan. 1993. Induction of apoptosis in fibroblasts by IL-1b-converting enzyme, a mammalian homolog of the *C. elegans* cell death gene *ced-3*. *Cell.* 75: 653–660.
46. Miyashita, T., and J. C. Reed. 1992. *bcl-2* gene transfer increases relative resistance of S49.1 and WEH17.2 lymphoid cells to cell death and DNA fragmentation induced by glucocorticoids and multiple chemotherapeutic drugs. *Cancer Res.* 52:5407–5411.
47. Monti, D., L. Troiano, F. Tropea, E. Grassilli, A. Cossarizza, D. Barozzi, M. C. Pelloni, M. G. Tamassia, G. Bellomo, and C. Franceschi. 1992. Apoptosis—programmed cell death: a role in the aging process? *Am. J. Clin. Nutr.* 55 (Suppl.) 1208S–1214S.
48. Nicotera, P., and S. Orrenius. 1992. $Ca^{2+}$ and cell death. *Ann. NY Acad. Sci.* 648:17–27.
49. Oltvai, Z. N., C. L. Milliman, and S. J. Korsmeyer. 1993. Bcl-2 heterodimerizes in vivo with a conserved homolog, Bax, that accelerates programmed cell death. *Cell.* 74:609–619.
50. Oppenheim, R. W. 1991. Cell death during development of the nervous system. *Annu. Rev. Neurosci.* 14:453–501.
51. Orrenius, S., D. J. McConkey, and P. Nicotera. 1985. Role of calcium in oxidative cell injury. Oxidative Stress, Stockholm, Sweden. 451 pp.
52. Owen, J. J. T., and E. J. Jenkinson. 1992. Apoptosis and T-cell repertoire selection in the thymus. *Annu. NY Acad. Sci.* 663:305–310.
53. Owens, G. P., W. E. Hahn, and J. J. Cohen. 1991. Identification of mRNAs associated with programmed cell death in immature thymocytes. *Mol. Cell. Biol.* 11:4177–4188.
54. Payne, C. M., and D. W. Cromey. 1991. Ultrastructural analysis of apoptotic and normal cells using digital imaging techniques. *J. Comput. Assisted Microscopy.* 3:33–50.
55. Pieper, R. O., B. W. Futscher, Q. Dong, T. M. Ellis, and L. C. Erickson. 1990. Comparison of O-6-methylguanine DNA methyltransferase (MGMT) mRNA levels in $Mer^+$ and $Mer^-$ human tumor cell lines containing the MGMT gene by the polymerase chain reaction technique. *Cancer Comm.* 2:13–20.
56. Putkey, J. A., K. F. Ts'ui, T. Tanaka, L. Lagace, J. P. Stein, E. C. Lai, and A. R. Means. 1983. Chicken calmodulin genes: a species comparison of cDNA sequences and isolation of a genomic clone. *J. Biol. Chem.* 258:11864–11870.

57. Radford, I. R. 1991. Mouse lymphoma cells that undergo interphase death show markedly increased sensitivity to radiation-induced DNA double-strand breakage as compared with cells that undergo mitotic death. *Int. J. Radiat. Biol.* 59:1353–1369.
58. Raff, M. C. 1992. Social controls on cell survival and cell death. *Nature (Lond.).* 356:397–400.
59. Raff, M. C., B. A. Barnes, J. F. Burne, H. S. Coles, Y. Ishizaki, and M. D. Jacobson. 1993. Programmed cell death and the control of cell survival: lessons from the nervous system. *Science (Wash. DC).* 262:695–700.
60. Richter, C. 1993. Pro-oxidants and mitochondrial $Ca^{2+}$: their relationship to apoptosis and oncogenesis. *FEBS (Fed. Eur. Biochem. Soc.) Lett.* 325:104–107.
61. Schwartz, L. M., and B. A. Osborne. 1993. Programmed cell death, apoptosis and killer genes. *Immunol. Today.* 14:582–590.
62. Screpanti, I., S. Morrone, D. Meco, A. Santoni, A. Gulino, R. Paolini, A. Crisanti, B. J. Mathieson, and L. Frati. 1989. Steroid sensitivity of thymocyte subpopulations during intrathymic differentiation. *J. Immunol.* 42:3378–3383.
63. Sentman, C. L., J. R. Shutter, D. Hockenbery, O. Kanagawa, and S. J. Korsmeyer. 1991. bcl-2 inhibits multiple forms of apoptosis but not negative selection in thymocytes. *Cell.* 67:879–888.
64. Sibley, C. H., and G. M. Tomkins. 1974. Isolation of lymphoma cell variants resistant to killing by glucocorticoids. *Cell.* 2:213–220.
65. Smith, C. A., G. T. Williams, R. Kingston, E. J. Jenkinson, and J. J. T. Owen. 1989. Antibodies to CD3/T-cell receptor complex induce death by apoptosis in immature T cells in thymic cultures. *Nature (Lond.).* 337:181–184.
66. Spear, B. T., and S. M. Tilghman. 1990. Role of a-fetoprotein regulatory elements in transcriptional activation in transient heterokaryons. *Mol. Cell. Biol.* 10:5047–5054.
67. Strasser, A., A. W. Harris, and S. Cory. 1991. *blc-2* transgene inhibits T cell death and perturbs thymic self-censorship. *Cell.* 67:889–899.
68. Woronicz, J. D., B. Calnan, V. Ngo, and A. Winoto. 1994. Requirement for the orphan steroid receptor Nur77 in apoptosis of T-cell hybridomas. *Nature (Lond.).* 367:277–281.
69. Wyllie, A. H. 1980. Glucocorticoid-induced thymocyte apoptosis is associated with endogenous endonuclease activation. *Nature (Lond.).* 284: 555–556.
70. Wyllie, A. H., J. F. R. Kerr, and A. R. Currie. 1980. Cell death: the significance of apoptosis. *Int. Rev. Cytol.* 68:251–306.
71. Yonish-Rouach, E., D. Resnitzky, J. Lotem, L. Sachs, A. Kimchi, and M. Oren. 1991. Wild-type p53 induces apoptosis of myeloid leukemic cells that is inhibited by interleukin-6. *Nature (Lond.).* 352:345–347.
72. Yuan, J., S. Shaham, S. Ledoux, H. M. Ellis, and H. R. Horvitz. 1993. The *C. elegans* cell death gene *ced-3* encodes a protein similar to mammalian interleukin-1b-converting enzyme. *Cell.* 75:641–652.